Cellular Responses to Photoreceptor Death in the *rd1* Mouse Model of Retinal Degeneration

Claudio Punzo and Constance Cepko

Purpose. Retinal degeneration is a disease that typically involves the loss of photoreceptors. Murine models have been established for such degenerations, and a variety of methods have been used to follow the progression of the disease. In the present study in situ hybridization was used to analyze gene expression responses in the different retinal cell types during the period of cone death in the *rd1* mouse model.

Methods. A preliminary microarray analysis led to the selection of 169 candidate genes that might change in level of expression during degeneration. Probes corresponding to these genes were used for in situ hybridization on tissue during the period of cone death. Expression values were assigned to the intensities of in situ hybridization signals and were compared between mutant and wild-type tissue.

Results. During the peak of cone death, the in situ hybridization signals were typically higher in the mutant. This signal change was often true of genes with a wild-type pattern of expression in ganglion cells, bipolar cells, and/or Müller glia. In such cases, the upregulation was highest in bipolar cells and/or Müller glia.

Conclusions. All retinal cell types responded during the process of retinal degeneration, as revealed by changes in gene expression. Genes that showed changes in the in situ hybridization signals during the period of cone death were typically higher in the mutant, with many of them expressed in both the ganglion cell layer and the inner nuclear layer. (*Invest Ophthalmol Vis Sci.* 2007;48:849–857) DOI:10.1167/iovs.05-1555

The vertebrate retina has highly specialized sensory neurons, the photoreceptors (PRs), which serve to initiate the process of vision. Cone PRs are responsible for vision during the brighter-light intensities of the day and mediate color vision.[1,2] Rod PRs are 1000 times more sensitive to light and initiate vision in dim light. In the human eye, light is focused onto a small region, the fovea, where high-acuity vision occurs. This area is highly adapted for daylight vision and contains only cone PRs. Approximately 95% of PRs in the rest of the retina are rods, with a central rod-rich ring that is almost free of cones.

Retinal degenerations (RDs) are retinal diseases often involving the loss of PRs. The disease with the largest number of affected individuals worldwide (20–25 million) is age-related macular degeneration (AMD), with a typical disease onset of >55 years of age.[3] Whereas AMD is thought to be caused by the interplay of environmental and genetic factors, other RDs appear to be the result of the simple Mendelian inheritance of a disease-causing allele. To date, 161 loci have been mapped, and for 112 loci, a specific gene has been linked to the disease (RetNet, http://www.sph.uth.tmc.edu/Retnet/ provided in the public domain by the University of Texas Houston Health Science Center, Houston, TX). Interestingly, a high percentage of RD genes are rod-specific, particularly in retinitis pigmentosa (RP), another late-onset RD. In cases in which the disease gene is rod-specific, rods die first, and then cone death follows, with kinetics depending on the particular disease. In humans, there is no RD known in which rods die and cones survive. Mutations in rod-specific genes thus appear to induce cone degeneration by mechanisms that are not intrinsic to cones. There are mutations in cone-specific genes that lead only to cone death.[4]

Naturally occurring mutations in animals, or experimentally engineered mice with RD, provide valuable models to study nonautonomous cone death. Although rodents have no macula, RD is similar to that in humans. Rod-specific mutations that have been found or introduced lead to rod death and subsequent cone death. One such model of RD is the *rd1* mutant mouse,[5] which carries a mutation of the rod-specific cGMP phosphodiesterase-β-subunit (*PDEβ*), which, when mutated, also causes RD in humans.[6]

The reasons for cone death in *rd1*, as in other forms of RD, remain a mystery. An important step in approaching this problem is to understand the changes that occur during rod and cone death. A well-described phenomenon is retinal remodeling, which occurs during periods of rod and cone death.[7–11] Although axonal arborization is first hypertrophic for certain inner nuclear layer (INL) cells during the period of rod death and bipolar (BP) dendrites start to disappear during the period of cone death, the INL and the ganglion cell layer (GCL) cells seem to survive in significant numbers. Thus the question arises, why do the other neurons in the retina survive when the majority of the PRs die? This question may be particularly apt for the murine models, as rods account for >70% of all retinal cells. It is thus of interest to characterize the response of retinal cells to PR death, to gain some insight into possible protective mechanisms that lead to the survival of cells of the INL and ganglion cell layer (GCL).

Little is known concerning how the different retinal cell types respond to the death of rods and cones in terms of gene expression. Models have been proposed for the cause of nonautonomous cone death, such as the loss of a trophic factor produced normally by rods and required for cone survival. Studies have provided evidence for such a factor, although proof that this accounts entirely for cone death is lacking.[12–16] Alternative models, in which dying rods either directly or indirectly lead to a toxic situation for cones, perhaps via the reactions of cells that are intimate with PRs, such as Müller glia (MG), can also be entertained.

Recent studies have applied microarray and proteomics technologies to characterize gene expression during rod and cone death in mouse models with a rod-specific mutation.[17–20] Although these studies provide a catalog of candidate genes,

From the Department of Genetics, Howard Hughes Medical Institute, Harvard Medical School, Boston, Massachusetts.

Supported by National Eye Institute Grant R01 EY014466, by Merck, and by an EMBO (European Molecular Biology Organization) fellowship to CP.

Submitted for publication December 7, 2005; revised July 20 and September 8, 2006; accepted December 1, 2006.

Disclosure: **C. Punzo**, None; **C. Cepko**, None

The publication costs of this article were defrayed in part by page charge payment. This article must therefore be marked "*advertisement*" in accordance with 18 U.S.C. §1734 solely to indicate this fact.

Corresponding author: Constance Cepko, Harvard Medical School, Department of Genetics, Howard Hughes Medical Institute, 77 Avenue Louis Pasteur, Boston, MA 02115; cepko@genetics.med.harvard.edu.

interpretations often remain limited because of the lack of information concerning the cellular locus of expression. To gain more insight into the responses of different retinal cell types in RD, as well as create a list of genes that respond and perhaps influence either the nonautonomous cone death or the survival of non-PR retinal cells, we undertook a screening of the cellular expression patterns of genes that change in *rd1*. Genes were selected by means of a preliminary screening via microarray analysis, and the gene expression patterns were compared between mutant and wild-type (wt) tissue during cone degeneration. The genes which showed a change in expression intensity during cone death were more likely to be upregulated and were expressed throughout the INL and the GCL of the mutant retina. Such genes often were most highly upregulated in BP cells and/or MG.

Material and Methods

Animals

Wt mice (C57Bl/6N) and mutant *rd1* mice (FVB/N) were purchased from Taconic Farms (Germantown, NY). Congenic FVB mice were purchased from Jackson Laboratories (stock number 4828l; FVB.129P2-Pde6b^{+} Tyr$^{c\text{-}ch}$/AntJ; Bar Harbor, ME). All procedures involving animals were in compliance with the ARVO Statement for the Use of Animals in Ophthalmic and Vision Research.

Molecular Methods

All experimental procedures performed with ready-to-use reagents were performed according to the manufacturer's instructions, if not otherwise stated. RNA extractions were performed (TRIzol; Invitrogen, Carlsbad, CA) and quality was assessed (model 2100 Bioanalyzer; Agilent Technologies, Palo Alto, CA).

Real Time PCR

Total RNA was extracted at the time points indicated in the Results section. One microgram of total RNA per time point was used for reverse transcription (Transcriptor; Roche, Indianapolis, IN). RT-PCR was performed (Light Cycler 2000; Roche) with DNA Master SYBR Green I reagents (Roche). The following primers were used for the RT-PCR: *Opn1sw* forward 5′-AAAGGCTGAACGGGAG-3′; *Opn1sw* reverse 5′-ACACGTCAGATTCGTCT-3′; rhodopsin forward 5′-TGCCAATATGCCCAC-3′; rhodopsin reverse 5′-GTACCCCATAGTTCCTGT-3′; *Gapdh* forward 5′-TCGGTGTGAACGGATT-3′; *Gapdh* reverse 5′-AAGACGCCAGTAGACT-3′. Conditions for the RT-PCR were as follows: *Opn1sw* 95° for 2 seconds, 51° for 10 seconds, and 72° for 25 seconds and rhodopsin and *Gapdh* 95° for 0 seconds, 61° for 10 seconds, and 72° for 20 seconds. Each experiment was performed in triplicate, and the data were averaged.

Rd1 Library

The *rd1* library was generated from 5-week-old *rd1* retinal RNA. The cDNA library was generated and cloned (pBluescript II XR; cDNA Library Construction Kit manual; cat no. 200455; Stratagene, La Jolla, CA).

Microarray Analysis

RNA extractions were performed at postnatal days (P)42 and P63. Hybridizations and slide scanning were performed with a kit according to the manufacturer's instructions (Genisphere, Hatfield, PA, as described by Corbo and Cepko[21]). Total RNA was extracted from five animals and pooled, and 3 μg of the total RNA was used per probe and hybridization. Experiments were performed in duplicate for each time point and array type. Because only one dye per slide, time point, and array was used, four slides per time point and array type were necessary to perform the experiments in duplicate, two for the wt and two for the *rd1* mouse. Thus, a total of eight slides were used per array for the two time points. The microarray analyses were performed on customized cDNA arrays. One microarray contained a retinal EST collection created by Bento Soares (University of Iowa, Ames, IA) encompassing 12,679 cDNAs, referred to here as the 12K array. These ESTs came from wt retinas. Thus, disease-specific genes that are not expressed at significant levels in wt retina are unlikely to be found on such an array. To account for such genes, RNA was extracted from 5-week-old *rd1* retinas, and a cDNA library was made. The library was transformed into bacteria to generate a collection of 17,328 clones. Because the library is unsequenced, a prescreening was conducted to select only those clones that change during degeneration. The 17,328 clones were hybridized with 5-week-old *rd1* and wt retinal RNA. From the library, 2610 genes were selected that showed potentially significant changes during degeneration. In addition to these genes, 1230 genes from either a laboratory collection of known retinal cDNAs or from an older version of a customized laboratory array (mouse brain ESTs: Bento Soares) were used to generate a minichip of 3840 cDNAs. Both the 12K array and the minichip were then used to select genes for the ISH analysis. A summary of the final 169 genes (123 from the 12K array and 46 from the minichip) selected for the ISH study is presented in Supplementary Table S1 (all supplementary tables are online at http://www.iovs.org/cgi/content/full/48/2/849/DC1). Genes of the 12K array were selected according to the following criteria: First, the average of the signal intensity of the duplicates had to be at least 1000 at one time point, either in the mutant or in the wt. Second, the change had to be more than twofold at both time points examined. This reduced the list to 283 for the genes that were higher in expression in wt and 9 for those that were lower. The list of genes that were higher in the wt comprised primarily PR genes. This list was reduced by removing known PR genes. The list of downregulated genes was increased by clustering (Cluster3 software; Eisen Laboratory: http://rana.lbl.gov/EisenSoftware.htm) the genes that passed the first criteria. This allowed an examination of a more comparable number of up- and downregulated genes. Only genes that clustered closest to the original nine downregulated genes were chosen. Some of the genes chosen through clustering had ratios of >2, but not at both time points, and thus were not picked up by the first selection criterion. A final list of 123 genes was compiled from the 12K array (Supplementary Table S1). Genes from the mini-chip were selected by using a method similar to the one used for the 12K array. The signal intensity was reduced to 500 because of the smaller range between the maximum and minimum signals. Because no sequence information was available at the time the microarray analysis was conducted, only a small number of genes was used for the ISH ($n = 46$). Meanwhile in a combined effort with the National Eye Institute (NEI) roughly 50% of the 2610 clones from the *rd1* library have been sequenced. The sequences are available in the public domain at the National Center for Biotechnology Web page (www.ncbi.nlm.nih.gov) with accession numbers ranging from DW711190 to DW712659.

Histologic Methods

TUNEL. TUNEL analysis was performed with kit (In Situ Cell Detection Kit; Roche) on 14-μm paraffin-embedded tissue sections. The procedure was the same as the one used for the ISH up to the rehydration in PBS; afterward the manufacturer's instructions were followed.

Cell Counting. Cell counting was performed as described (Young and Cepko[22]). Cells were detected with a Cy3-α-mouse antibody (Jackson Immunoresearch Laboratory) and counterstained with 4′,6′-diamino-2-phenylindole [DAPI]. A minimum of five retinas was analyzed with a total cell count of 2000 cells.

X-gal Histochemistry. X-Gal staining was performed according to standard procedures.[23] Retinas were fixed for 15 minutes and stained at room temperature overnight.

In Situ Hybridization. Section ISH was performed on 14-μm paraffin-sections. In brief, the retinas were dissected in PBS, fixed for 30 minutes in 4% PFA/PBS, washed three times for 10 minutes each in PBS, dehydrated in a series of increasing ethanol (EtOH) concentra-

tions (25%, 50%, 75% EtOH/H_2O and 2× 100% EtOH 10 minutes each) cleared two times for 5 minutes each in xylene, transferred for 20 minutes in a 1:1 mixture of xylene:paraffin (65°C), washed three times for 20 minutes each in paraffin (65°C), and incubated overnight at 65°C in paraffin. After mounting and sectioning, the slides were dried overnight at 37°C and stored at 4°C until used. Before rehydration of the tissue, the slides were heated at 65°C for 1 hour, cooled quickly, and rehydrated two times for 5 minutes each in xylene, two times for 5 minutes each in EtOH, and then in decreasing concentrations of ethanol to increasing PBS concentrations for 5 minutes each. The sections were fixed (4% PFA/PBS) for 10 minutes, washed three times for 5 minutes each in PBT (PBS 0.1% Tween-20), proteinase K treated for 10 minutes (1 μg/mL), washed two times for 5 minutes each in PBT, postfixed in 4% PFA/PBS for 5 minutes, washed three times for 5 minutes each in PBT, acetylated for 10 minutes (0.1 M triethanolamine/25 mM acetic acid anhydrid), washed three times for 5 minutes each in PBT, air dried for 10 minutes, and prehybridized for 1 hour in hybridization buffer (10 mM Tris [pH 7.5], 0.6 M NaCl, 1 mM EDTA, 0.25% SDS, 10% dextran sulfate, 1× Denhardt's, 200 μg/mL yeast tRNA, and 50% formamide). Hybridizations were performed overnight at 70°C. Riboprobes were synthesized from 300 ng PCR (T3/T7) product of the ESTs described in Supplementary Table S1 and labeled using digoxigenin-tagged UTP (Roche). RNA synthesis was performed in a total of 20 μL. After synthesis, the probe was treated for 15 minutes with DNase (RNase free; Roche), precipitated, washed with 70% EtOH, air dried, and resuspended in 100 μL H_2O. Three of 100 μL probes were used in 150-μL hybridization buffer. The following day, cover slips were removed in 5× SSC, and the slides were washed for 30 minutes in 1× SSC/50% formamide at 65°C, 10 minutes in TNE (10 mM Tris [pH 7.5], 500 mM NaCl, and 1 mM EDTA) at 37°C, 30 minutes in TNE+RNaseA (20 μg/mL; Roche) at 37°C, 10 minutes in TNE at 37°C, 20 minutes in 2× SSC at 65°C, and two times for 20 minutes each in 0.2× SSC at 65°C. The slides were then washed in MABT (100 mM maleic acid, 150 mM NaCl, and 0.1% Tween; pH adjusted to pH 7.5) two times for five minutes each, blocked for 30 minutes in MABT+20% heat-inactivated sheep serum, incubated 2 hours in blocking solution+ α-digoxigenin-alkaline-phosphatase (1:2500; Roche), washed three times for five minutes each with MABT, and then detected with NBT/BCIP (5-bromo-4-chloro-3-indoyl phosphate–nitroblue tetrazolium; Sigma-Aldrich, St. Louis, MO). The ISH experiments are shown as supplementary figures, available online at http://www.iovs.org/cgi/content/full/48/2/849/DC1, named according to the clusters for their wt expression values (clusters 1–8). The distribution of the 169 genes into their respective clusters is shown in Supplementary Table S2.

Results

Characterization of the Kinetics of PR Cell Death

The death of rods and cones in the *rd1* mutant mouse model has been studied previously.[24,25] Rod death takes place primarily during the second and third postnatal weeks. Cone death is clearly visible from the fifth postnatal week, and continues for many months. To precisely determine the kinetics of rod and cone death for future analysis by microarray and ISH, three different approaches were used. First, TUNEL analysis was performed on paraffin-embedded sections from each postnatal day between P0 and P20, and then for every week up to postnatal week 10. At P11, many TUNEL-positive cells were found, with a peak observed at P12. The number then diminished, with a central-to-peripheral gradient over time (Supplementary Figs. S1A–E, http://www.iovs.org/cgi/content/full/48/2/849/DC1). By P20, few TUNEL-positive cells were observed, and these were primarily in the periphery (Supplementary Fig. S1D). A later central-to-peripheral gradient of TUNEL-positive cells was observed between postnatal weeks 4 and 10 (Supplementary Figs. S1F–H). These two waves of cell death, between P10 and P20, and postnatal weeks 4 and 10, most likely coincide with the major rod and cone death periods, respectively, as previously observed.[25]

Second, quantitative real-time PCR was performed to measure the loss of a rod- and cone-specific RNA species. RNA of mutant and wt retina from different time points was analyzed for either rhodopsin or *Opn1sw* (Opsin1 short wave length is also referred to as blue cone opsin). Since the TUNEL analysis showed no significant number of $TUNEL^+$ cells up to P10, RNA was extracted from P10 and every other day up to P20, and then every week up to postnatal week 11. Primers specific for the housekeeping gene, *Gapdh*, were used as a control for the amount of total RNA. Concordant with the TUNEL analysis and the DAPI staining of sections (Supplementary Fig. S1), a rapid decrease in rhodopsin transcript was observed from P10 to P20 (Fig. 1A). After P20, the rhodopsin transcripts reached a low level, which was stable over the remaining period, reflecting a small number of rods still present in the periphery of the retina.[25] The initial increase of rhodopsin transcript in wt retinas from P10 to P16 is due to the postnatal maturation of the retina.[26,27] The blue opsin transcript levels in the *rd1* mutant started to diverge from the wt samples only after P35, and continued to descend until P70 (Fig. 1B). The initial increase followed by a decrease in wt retina correlates with the fact that the gene is expressed initially throughout the entire retina and is then downregulated in the dorsal retina.[28,29]

In a third method of quantifying rod death, we used a rod-specific antibody. Retinas were dissociated at different time points, and cells were plated onto slides and stained with a monoclonal α-rhodopsin antibody. A linear decrease in rhodopsin-positive cells was observed, suggesting that, at any given time, the percentage of dying rods was the same (Fig. 1C).[30] Because the total percentage of cones is very low in the mouse retina and the changes occur over an extended period, cone death was monitored by means of a cone-specific *lacZ* line that was crossed into a *rd1* mutant background. This line expresses β-galactosidase under the control of the human red-green opsin promoter but is expressed in all cones of the murine retina.[31] This approach allowed a territorial rather than a quantitative assessment of cone death. No difference was observed between wt and *rd1* retinas up to P21. A clear loss of X-gal staining was observed at P28, with a central-to-peripheral gradient (Fig. 2). At P77, cones were mainly present in the periphery, with a few patches in more central regions (data not shown for time points between the 4th and 11th weeks).

The foregoing analysis of rod and cone death was used to choose the microarray analysis time points of P42 and P63. Both time points were selected because both are during the period of major cone death, but after major rod death, and thus changes associated with cone death might be apparent (Fig. 1B). The ISH analysis was performed at P35. This time point was selected because cone death is ongoing (Fig. 2C), but the central-to-peripheral gradient of cone loss is such that central-to-peripheral changes in gene expression would be apparent.

ISH Analysis

RNA samples from *rd1* and wt were applied to cDNA microarrays comprising cDNA collections enriched for expression in the retina and the nervous system. Genes showing changes in levels of expression were selected for analysis by ISH (see the Material and Methods section). The 169 genes chosen from the microarray analysis were almost evenly distributed between genes that were higher in wt versus mutant and those that were higher in mutant versus wt. To minimize the variables of an ISH analysis, and make the results as quantitative as possible, retinas from *rd1* and C57Bl/6N were mounted into the same paraffin block. Each slice had two different sections. A ribbon of 8 to 10 slices was transferred onto one slide generating 16 to

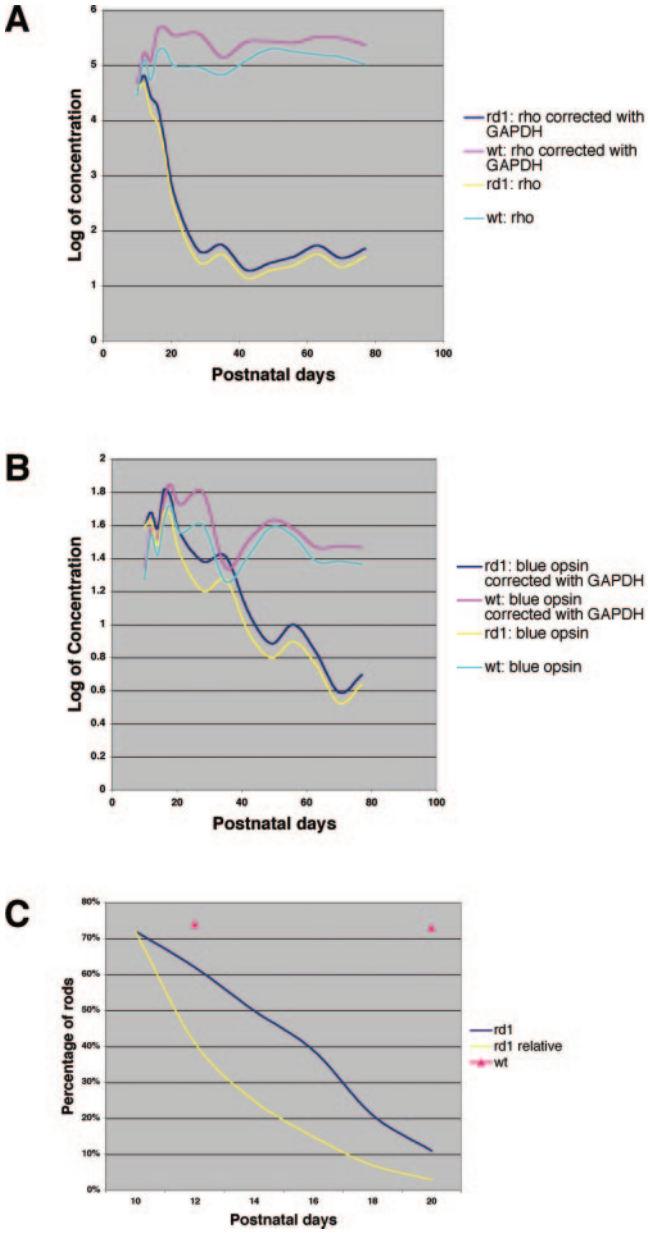

FIGURE 1. Real time PCR (RT-PCR) analysis for rhodopsin and *blue cone opsin* during rod and cone cell degeneration. (**A**) RT-PCR for rhodopsin transcripts and (**B**) for *blue cone opsin* over time. Curves in yellow and turquoise represent uncorrected raw data and curves in blue and pink are data normalized to the housekeeping gene glyceraldehyde-3-P-dehydrogenase (*Gapdh*). (**C**) Percentage of rods during rod degeneration. Retinas were dissociated at multiple time points. Rods were identified by α-rhodopsin antibody and total cells by nuclear DAPI staining. *Blue curve*: percentage of the actual count of rhodopsin-positive cells per total cells; *yellow curve*: percentage based on a correction to the total number of cells of a wt retina. (**C**) *Pink triangles*: percentage of the actual count on wt retinas at the time points indicated. *x*-axis: postnatal days; *y*-axis the logarithm of the relative concentration (**A**, **B**) or percentage of rhodopsin-positive cells (**C**). (*rd1*) FVB/N mutant mice. (wt) Wild-type C57Bl/6N mice.

20 sections per slide, which were then hybridized with a single probe. A set of two pictures was used for the analysis, and was taken from the same slide with the same exposure for a given probe. If no specific central to peripheral pattern was observed, the picture was taken from a central region. To compare the large amount of ISH data systematically, a method was devised that is similar to that used previously for the developing retina.[32] Expression values of 0 to 5 were assigned by visual inspection, as was the location of the ISH signal. The values were assigned for each of the seven retinal cell types; GC, amacrine cell (AC), horizontal cell (HC), BP, MG, rod, and cone) and for the inner segments (IS) of photoreceptors by direct inspection of each panel. A value of 0 was assigned if the cell type was absent. That was the case only for rods in the mutant tissue. The analysis of the two panels for a given probe was performed in parallel in one session. The translation of the ISH patterns into expression values at cellular resolution was based on the cell types that are normally located in the region of the retina where the ISH signal was seen. This was sometimes straightforward, but also presented the following problems. First, RNAs can be located in subcellular regions that are distant from the cell body. This is often seen for rod and cone genes, which show ISH signal in the IS. Nonetheless, this was mostly straightforward to interpret, since the only other cell type with processes in that region are MG cells. Their processes span the entire retina, engulf almost every retinal cell type, and form the outer limiting membrane and inner limiting membrane, confusing assignments not only of rods and cones, but also of GCs and INL neurons. Similarly, subcellular localization of RNA into neuronal processes of INL cells can produce a diffuse pattern in the INL and inner plexiform layer, which complicates the interpretation. In addition, there are several ACs that are displaced into the GCL, so that signal in the GCL could be due to these ACs. Thus, the assignments to a cell type are tentative, but were made to simplify the discussion of the data and provide a starting point for an understanding of cellular responses.

Cellular Gene Expression Changes during RD

Cellular expression levels observed by ISH were compared between wt and mutant by subtracting the mutant expression

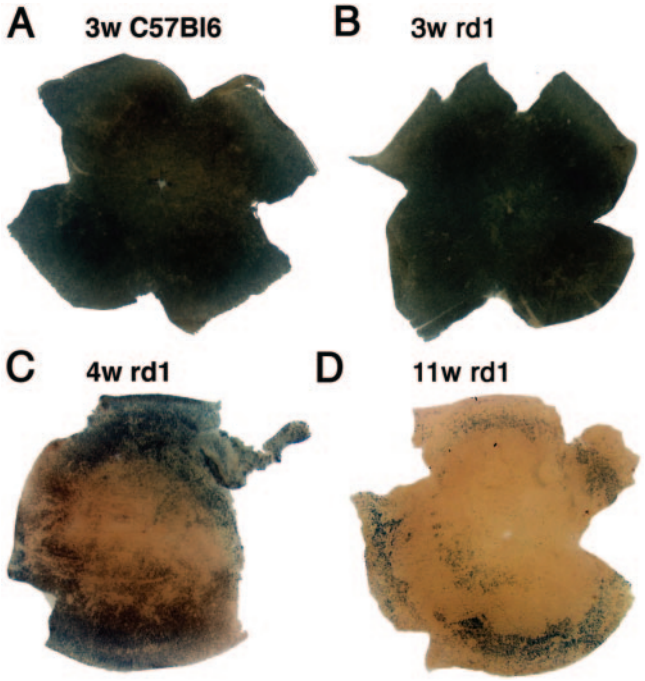

FIGURE 2. Cone degeneration in *rd1* mice. Cones were monitored by use of a cone cell-specific promoter (human red-green opsin promoter[31]) driving the expression of β-galactosidase. (**A–D**) X-gal staining of wholemount retinas. (**A**) Wt retina. (**B–D**) *rd1* retina. Postnatal time is indicated in weeks (w) at the *top* of each panel.

values for a given cell type and probe from the corresponding wt values (e.g., wt GC − *rd1* GC). The advantage of subtracting the values rather than calculating ratios is that large data sets can be manipulated without the problem caused by division by 0. If the difference was >0, the gene was expressed at a higher level in the particular cell type of a wt retina, and if it was <0, it was expressed at a higher level in the cell type of the mutant retina. The analysis of genes expressed in GCL showed that, at P35, during major cone death, two times more genes had values <0 than had values >0 (Fig. 3A).

Genes expressed in the INL were tentatively assigned to ACs, HCs, BP, and MG via the location of the signal within the INL. The tendency for genes that changed in ACs and HCs was similar to that seen for genes of the GCL, but the difference between the number <0 and >0 was less significant (1.4-fold), suggesting that in ACs and HCs, a similar number of genes is up- or downregulated during PR death (Fig. 3A). In contrast to the ACs and HCs, the number of genes expressed in MG and BP with values <0 showed a significant increase (5.4-fold and 5.5-fold, respectively).

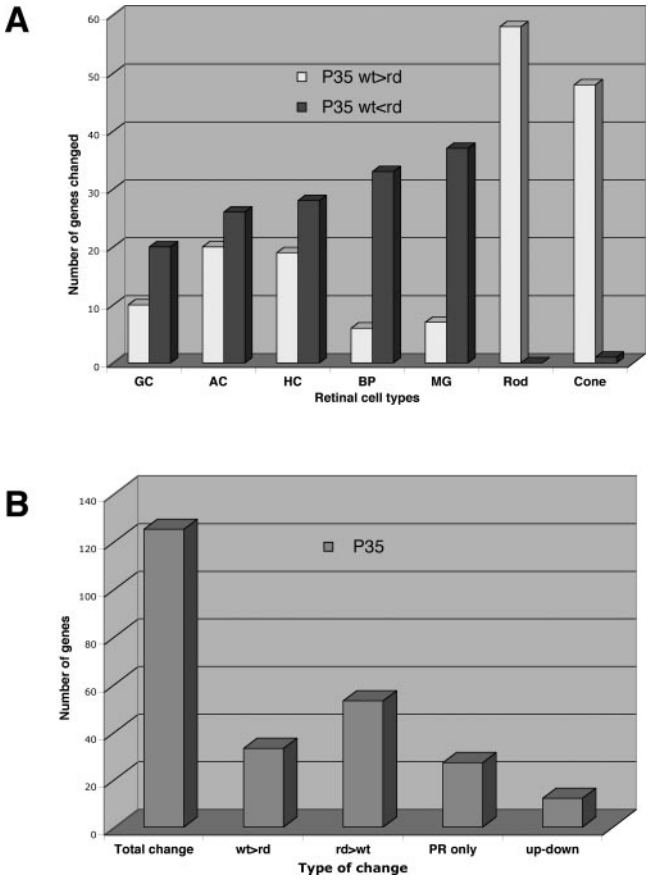

FIGURE 3. Summary of gene expression changes during RD. (**A**) Summary of cellular changes. The expression values in the corresponding cell types between C57Bl/6N and *rd1* were subtracted. Values >0 (wt>*rd1*) indicate that the gene is expressed at higher levels in wt tissue, whereas values <0 (wt<*rd1*) indicate that the gene is expressed at higher levels in the *rd1* retina. Plotted on the *y*-axis is the total number of genes that changed. (**B**) Number of genes changing. (Total change): Total number of genes that changed. (wt>rd) Number of genes that were exclusively expressed at higher levels in wt retinal cells. (*rd*>wt) Number of genes that were exclusively expressed at higher levels in *rd* retinal cells. (PR only) Number of genes that changed only in PR. (up-down) Number of genes that were expressed at higher and lower levels in different retinal cell types. (The sum of wt>*rd*, *rd*>wt, PR only and up-down is equal to the total changes).

Although many known PR genes that showed changes on the microarray analysis were not screened by ISH, some genes with microarray changes that were similar to the known PR genes turned out to be enriched in the PR. Genes expressed in rods were always at higher levels in wt retinas (Fig. 3A) as no rods were present in the mutant retinas at P35. Because the expression value assigned for an absent cell type was 0, the difference between wt and mutant values were always >0. In contrast to rods, expression values in cones reflect gene expression changes, as there are still cones present in *rd1* retinas at P35. The analysis of cone gene expression levels by ISH showed that 48:1 genes had expression values >0, suggesting that gene expression in cones during this period was globally reduced, perhaps reflecting the fact that many cones are dying (Fig. 3A). Thus, the observations of the ISH patterns agree with the disease pathology of cone death. (A summary of all the genes that changed and the cells involved is presented in Supplementary Table S3).

As the expression of a given gene was often complex, occurring in more than one cell type, a comparison was made of the levels of expression in the different cell types in wt and *rd1*. For example, a certain gene could demonstrate higher expression levels in wt GC and MG cells, while at the same time the gene may have higher expression levels in other cell types (e.g., ACs and HCs) of the mutant retina. This analysis showed that of the 125 genes that showed changes by ISH, 53 were expressed exclusively at higher levels in *rd1*, and 33 were expressed exclusively at a higher level in wt (Fig. 3B). Twenty-seven genes had exclusively PR-specific changes. Most of these genes are PR-specific, thus their change is due to the lack of rods in the mutant retina at P35. Twelve genes were expressed at higher levels in one cell type and at lower levels in another cell type. Overall, these data show that 90% (113/125) of all the genes that changed have unidirectional changes. Excluding those that were PR-specific, of the genes expressed in the INL and GCL, 87% showed unidirectional changes; they were either solely up- or downregulated in *rd1* or wt. Of these, 54% showed an upregulation in the mutant retina, 34% showed a downregulation, and 12% changed both ways. The results may suggest that the disease process similarly regulates the expression of a particular gene, even in different cellular contexts.

The changes in gene expression levels during cone death can be summarized as follows: During cone death, there is a higher level of expression in the GCL and the INL of the *rd1* retina, mainly due to an increase in expression levels in GCs, BP cells, and/or MG (Fig. 4). Changes in the ONL are due to a decrease in the number of rods and cones at the time point of the analysis. The results suggest that the genes assayed by ISH, whose levels are sensitive to RD and that are expressed in the GCL, are more likely to be expressed at higher levels during cone death. Genes that change in RD and are expressed in ACs and HCs during the peak of cone death change almost evenly in both directions. In contrast, among the genes assayed by ISH, BP (and possibly MG) significantly upregulate expression during the peak of cone death. Overall, GCL and INL cells are more likely to upregulate than downregulate gene expression during RD (54% vs. 34%).

Gene Expression Patterns of Genes That Change during RD

It was of interest to determine whether genes that changed in expression levels during RD exhibited particular gene expression patterns in wt. For example, genes that were upregulated in BP cells might be expressed in many cell types, but only be upregulated in BP, in response to RD. To search for patterns in the expression of genes that changed in RD, the cellular wt

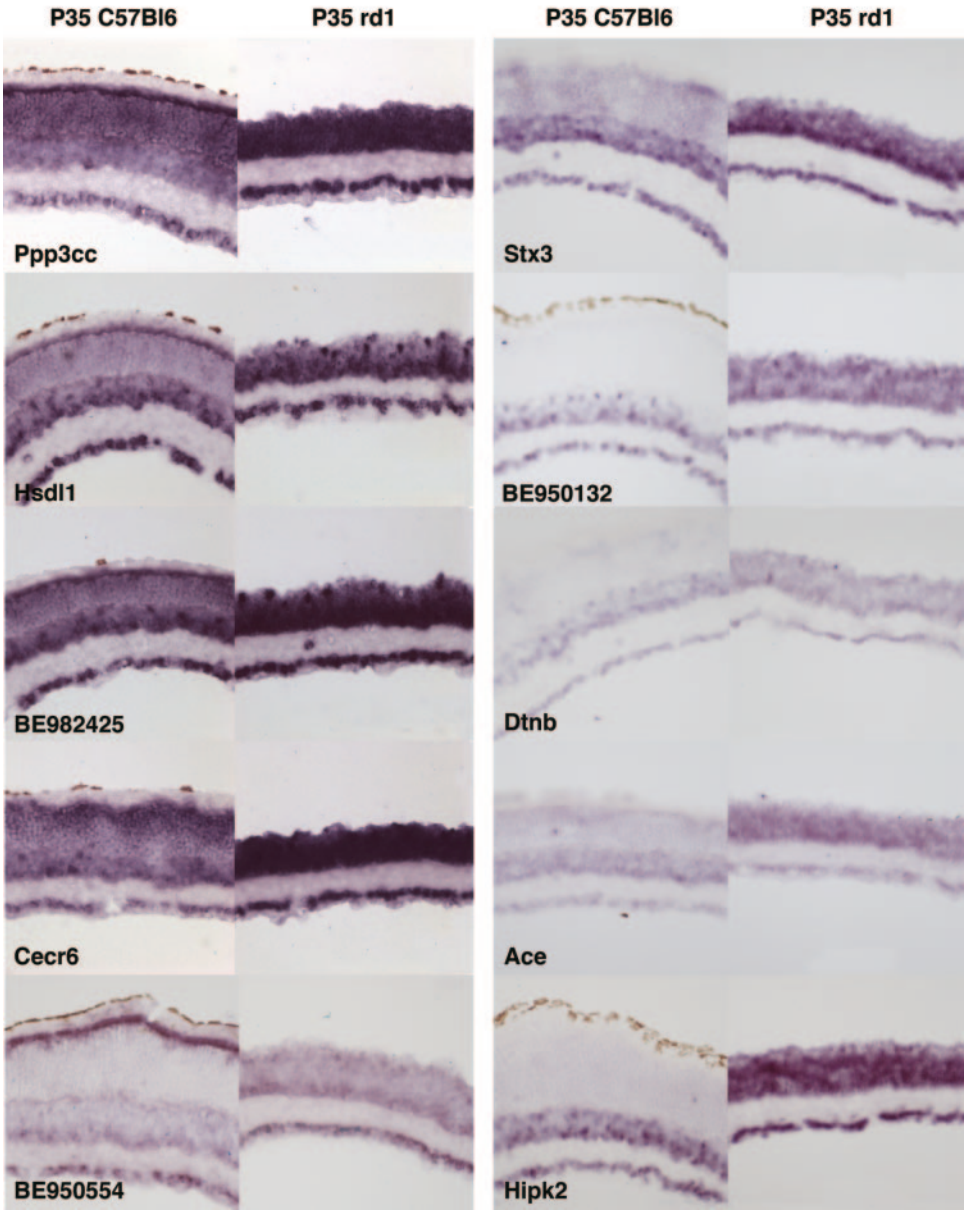

FIGURE 4. ISH for genes with higher expression levels in *rd1* versus wt retinas. Two columns of ISHs (10 genes total) are shown. On the left of each column is the wt and on the right the corresponding *rd1* section. The gene is indicated at the bottom *left* of the wt image.

values of the 169 genes were clustered. Eight clusters were defined and the genes were assigned to one of 8 clusters (clusters 1, ONL; 2, GCL, INL but no ONL; 3, GCL, INL, IS; 4, GC, AC, HC; 5, GC, AC, HC, IS; 6, panretinal expression; 7, a single cell type; 8, the rest of the genes that did not fall into any of the other 7 clusters; see also Supplementary Tables S2, S3). The relative percentile distribution of the 169 genes and of each of the five categories of changes presented in Figure 3B was calculated. Of the 169 genes, 125 showed changes by ISH and the 125 were distributed as follows: PR-only: 27 genes, wt>*rd1*: 33 genes, *rd1*>wt: 53 genes and up-down: 12 genes; Fig 5G).

The analysis shows that none of the expression patterns assigned to the 169 genes was overrepresented among the genes expressed at higher level in wt or at higher level in the mutant, or for genes that changed in both directions (bars in blue shades compared with yellow bars). An exception was the PR-specific changes (red bar), as PR genes are found only in clusters 1, 6, and 8, and thus those clusters are the only ones expected to have changes due to the loss of the ONL in *rd1*. Of note, clusters 4 and 5 account for >40% of genes that were upregulated in the mutant. Although both clusters have GC, AC, and HC expression patterns ± IS expression, one-third of such patterns resulted in upregulation in BP and/or MG. Because the expression level was either very low or absent in wt BP and/or MG, this response in *rd1* is due to either an ectopic upregulation (i.e., genes that initiate expression in BP and/or MG in response to RD) or a very strong upregulation for such genes in BP and/or MG, but not as strong an upregulation in the other retinal cell types.

A summary of the ISH analysis is as follows: Gene expression changes observed by ISH during cone cell death in the *rd1* mouse model were more likely to be due to upregulation in the mutant tissue. Regardless of whether a gene was up- or downregulated, 90% of the genes that changed did so in only one direction, even though the gene was typically expressed in more than one cell type. The cell types most affected were cells of the GCL, BP and/or MG. There were no specific wt expression patterns for the genes that changed, with the exception of the PR-specific genes.

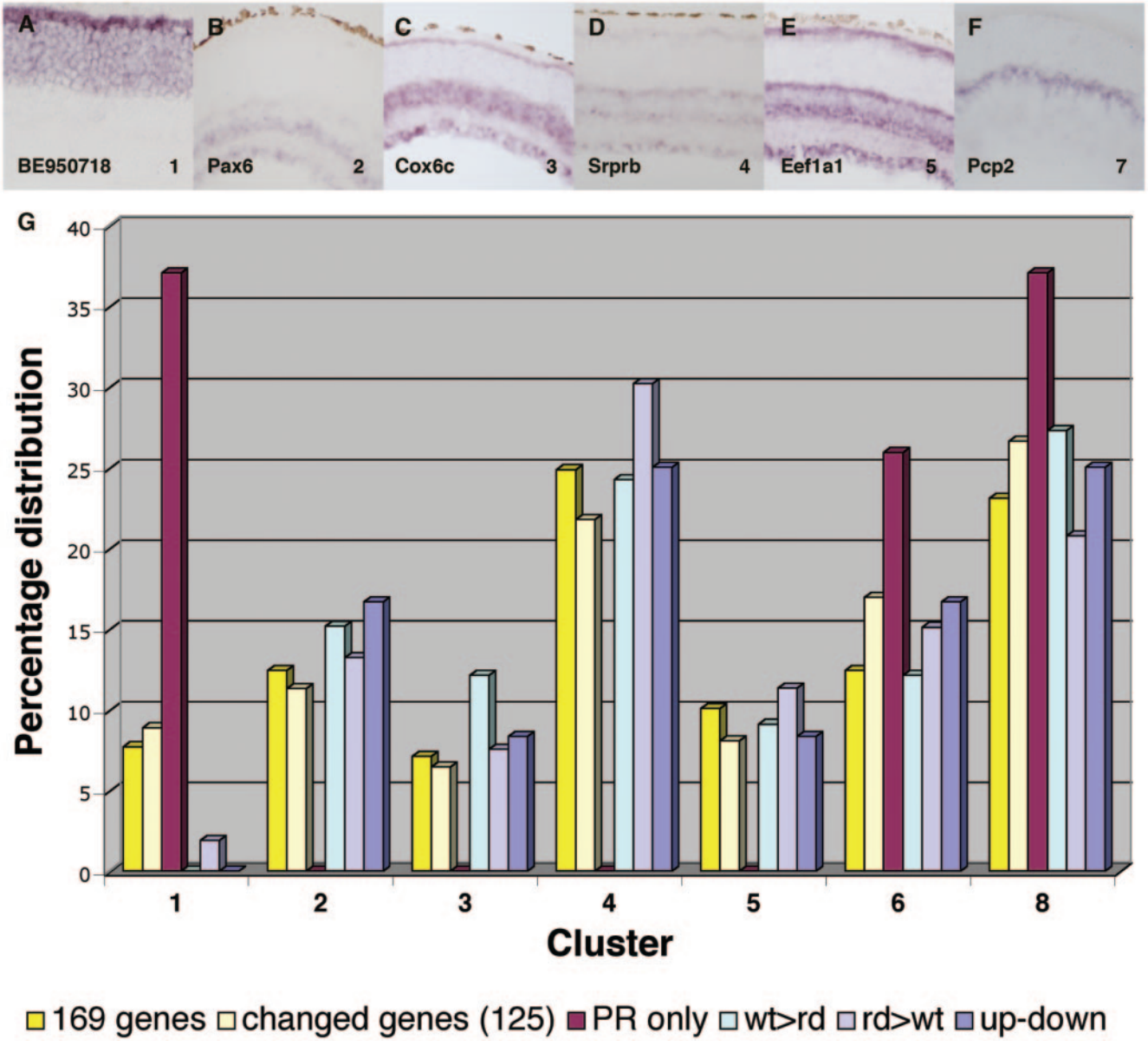

FIGURE 5. Percentile distribution of genes that change during RD. (**A–F**) show examples of ISH patterns in wt retinas at P35 of genes belonging to clusters 1 to 5 and 7, respectively (cluster number in lower right of each panel). The gene symbol is indicated in the panel. A list of all genes sorted into their clusters for wt expression patterns is found in Supplementary Table S2. (**G**) Relative percentile distribution of the genes that changed by microarray that were chosen for ISH (169 genes) and genes that showed changes by ISH (125/169 genes) within each cluster. The percentages are relative to the total number of genes that were expressed within each category of Figure 3B. Clusters: 1, ONL; 2, GCL, INL but no ONL; 3, GCL, INL, IS; 4, GC, AC, HC; 5, GC, AC, HC, IS; 6, panretinal expression; 7, one single cell type; 8, rest of genes that did not fall into any of the other seven clusters.

DISCUSSION

The primary goal of the study was to analyze the responses of different retinal cell types to RD. This is the first extensive study of the cellular locus of expression for genes that change during RD. Gene expression changes, as viewed through ISH, were used to measure these responses, with microarrays serving as the basis for the selection of genes for ISH. An EST library was generated from the *rd1* retinas at the time of major cone death, to provide access to clones that are not found in clone collections from wt animals. A well-characterized mutant, *rd1*, was chosen for this analysis. RT-PCR and single cell analysis gave a quantitative measure of cell death, and TUNEL and staining of a cone opsin-lacZ transgene revealed the topography of death. These studies clearly revealed two phases of PR death, in keeping with previous results.[24,25,33] During the second and third postnatal weeks, most of the rods died, resulting in an ONL with one cell layer in the central region of the retina, and two to three cell layers in the peripheral ONL. Whereas rods died in the periphery at the end of the third week, during the fourth week, a second wave of apoptosis started in the center, due to the death of cones.

ISH as a Comparative Tool

To compare the responses of different cell types to RD in a comprehensive manner, a method that was applicable to many different genes was required, e.g., antibodies are not available

to the large number of genes that are expressed in a tissue. ISH on tissue sections was thus chosen for this purpose. However, ISH is not typically a quantitative method. Different probes for the same gene can result in different signal intensities, perhaps due to different mRNA isoforms and/or secondary structures. In addition, some genes that appear to be low abundance by one method can result in strong ISH signal, and vice versa. Thus, expression levels of different genes are difficult to compare by this method. The ISH analysis presented herein neither compared expression levels of different genes to each other, nor compared different probes for the same gene. Rather, the results of hybridizing the same probe on different tissue sections on the same slide were compared. This allowed the ISH signals to be compared since the technical reasons for variability were controlled. In addition, several sections from each type of eye were present on the same slide. To ensure the best possible result, the values for the wt and mutant sections were assigned in the same session. For the reasons just mentioned, only values relative to each other within one slide were compared during the entire analysis.

The study was not performed in a congenic mouse background, and thus strain differences may complicate the interpretation of the data. A new congenic mouse strain generated by Jackson Laboratories was made available to us at the end of the study, allowing us to determine whether the results observed in the noncongenic strains would reproduce in a congenic FVB mouse background without the *rd1* allele. We mounted P35 wt (C57Bl/6N), FVB congenic, and *rd1* retinas into the same paraffin block, sectioned the retina, and performed ISH with 18 genes. Fourteen of these genes showed the same changes in wt (C57Bl/6N) and the FVB congenic when compared to *rd1*. Thus, the majority of changes observed by ISH at P35 between wt (C57Bl/6N) and *rd1* are likely to reflect the progression of the disease, as opposed to strain differences. Nonetheless, caution is advised in interpreting changes of any individual gene, as roughly 20% of the genes tested in a congenic background failed to show mutation-specific changes. Additional caution is advised when comparing gene expression in noncongenic mouse strains during development. We performed this same study at earlier time points (P10, P12), using both microarrays and ISH to compare expression between C57Bl/6N and FVB. Although many genes changed, we found that a later comparison of these genes in the congenic strain showed that most of the changes were due to strain differences. We presume that slightly different kinetics of development in different strains can lead to such differences.

Cellular Responses to Cone Death in RD

Understanding changes on a cellular level during the cone death phase of PR degeneration can promote our understanding of the disease state in at least two ways. The localization of changes to individual cell types points to which cells are responding during cone death. Identifying the localization may give insight into the stimuli for such changes (i.e., the signals released by compromised cones, and/or protective mechanisms used by cells that survive the large amount of neuronal death in RD). The identification of cellular responses and gene functions may help us understand what metabolic or pathologic processes are going on in different cell types during the cone death phase. This study shows that GCs, BP, and possibly MG react the most during cone death. In many cases, the expression in BP and/or MG showed a greater induction than in the other INL cell types. In age-matched wt retina, the expression pattern of such genes was often a GC, AC, and HC pattern, suggesting that the induction in MG and BP cells may be ectopic, or at least is a very strong induction.

It is fair to question to what extent these findings are representative of the disease process, versus a reflection of our selection process for genes to screen by ISH. The microarray analysis performed was used as a screen to select genes that potentially change, as picking them randomly from a retinal library would probably have yielded fewer changes. If we compare the distribution of the genes in the different ISH categories (wt up; rd up; up-down; PR-only and no change; see Fig. 3B) to the *x*-fold change of the microarray study, no correlation could be found except for the PR-only genes. This notion may seem counterintuitive, but may be predicted based on the changes that occur during the process of RD. Most PR-enriched or -specific genes would be at lower levels in the *rd1* RNA samples. As these genes are not informative regarding the cellular responses of non-PR cells to the disease process, most of the known PR genes were not screened by ISH. In addition, the RNA preparation of *rd1* would be significantly enriched for genes that are expressed selectively in the GCL and/or INL, because ~70% of the cells from the ONL are absent from the *rd1* RNA sample. It is thus difficult to recognize the microarray results that point to the genes that are specifically induced in the GCL and or INL. In addition, it is possible that the different time points used for the microarray analysis and the ISH analysis led to some different outcomes. However, we feel that this is unlikely as we scanned over the entire central–peripheral extent of each section, which would reveal temporal differences over a range of ages. Finally, because genes can change in different cell types in different directions, and to different extents in different cell types, changes seen by ISH may not be seen, or may be seen to the same degree, in the microarray data. Nonetheless, by using microarray-detected x-fold changes to guide the selection of genes for ISH analysis, we were able to choose a set of genes in which the majority showed changes by both methods (125/169). The most rigorous way to determine whether the 169 genes chosen for ISH screening in the current study was an unbiased selection of genes would be to compare these data to the results from a random selection of cDNA clones from retinal libraries.

The differences observed in the cellular responses to cone death raise two questions. First, why are the changes in gene expression mainly upregulation in GCs, BP cells and/or MG, whereas in ACs and HCs the changes seem to be more uniformly distributed between up- and downregulated genes? Second, are these observations an *rd1*-specific phenomenon, or are they common to other RD models? The latter question can be answered by analyzing different mouse models of RD, using probes for the same set of genes.

Types of Genes That Change in RD

A gene ontology analysis of the genes that change during RD has the potential to provide some insight into the nature of the responses in the different cell types. However, we characterized a relatively small number of genes that changed via ISH, and the fact that molecular functions and biological processes are assigned to only roughly 50% of genes make this a speculative exercise. Of the 53 genes that were upregulated in *rd1*, only 31 were annotated. Similarly, of the 33 genes downregulated in *rd1*, 19 were annotated, and 5 were annotated of the 12 that were up- and downregulated in different cell types. In total, 57 genes were annotated (Supplementary Table S4) out of the 98 genes that changed by ISH (excluding the PR enriched/specific genes). The class with the highest representation was signal transduction in cell–cell communication, with 19 genes (10 up- and 8 downregulated in *rd1* and 1 up- and downregulated). This finding may suggest an increase in cellular crosstalk during cone death. The other classes with high representation were metabolism (8:7:0 respectively), transcriptional regulation (6:2:0, respectively), and transporter proteins (mostly channels; 4:2:2, respectively). The number of genes

found in energy metabolism and transporter activities suggests a restructuring of the remaining tissue during cone death and a change in energy supply. Retinal remodeling is a well-studied phenomenon in the *rd1* mutant.[7,34] BP cells may respond during cone death, as by then they have lost both rod and cone presynaptic partners. MG may be affected, as they normally supply the retinal neurons with energy or growth factors.[35] As the energy supply chain via the retinal pigmented epithelium to photoreceptors and the oxygen supply to MG may have been altered by the degeneration of rods and cones, they may need to change their expression profile to adapt to the new environment.

Acknowledgments

The authors thank Jeremy Nathans for the cone-lacZ line, Jeff Trimarchi, Rahul Kanadia, Karin Roesch, and Diana Esshaki for a critical reading of the manuscript, and Soledad Jorge for technical help.

References

1. Collin SP, Trezise AE. The origins of colour vision in vertebrates. *Clin Exp Optom*. 2004;87:217–223.
2. Nathans J. The evolution and physiology of human color vision: insights from molecular genetic studies of visual pigments. *Neuron*. 1999;24:299–312.
3. Chopdar A, Chakravarthy U, Verma D. Age related macular degeneration. *BMJ*. 2003;326:485–488.
4. Yang RB, Robinson SW, Xiong WH, Yau KW, Birch DG, Garbers DL. Disruption of a retinal guanylyl cyclase gene leads to cone-specific dystrophy and paradoxical rod behavior. *J Neurosci*. 1999; 19:5889–5897.
5. Bowes C, Li T, Danciger M, Baxter LC, Applebury ML, Farber DB. Retinal degeneration in the rd mouse is caused by a defect in the beta subunit of rod cGMP-phosphodiesterase. *Nature*. 1990;347: 677–680.
6. McLaughlin ME, Sandberg MA, Berson EL, Dryja TP. Recessive mutations in the gene encoding the beta-subunit of rod phosphodiesterase in patients with retinitis pigmentosa. *Nat Genet*. 1993; 4:130–134.
7. Strettoi E, Pignatelli V, Rossi C, Porciatti V, Falsini B. Remodeling of second-order neurons in the retina of rd/rd mutant mice. *Vision Res*. 2003;43:867–877.
8. Strettoi E, Porciatti V, Falsini B, Pignatelli V, Rossi C. Morphological and functional abnormalities in the inner retina of the rd/rd mouse. *J Neurosci*. 2002;22:5492–5504.
9. Marc RE, Jones BW. Retinal remodeling in inherited photoreceptor degenerations. *Mol Neurobiol*. 2003;28:139–147.
10. Gouras P, Tanabe T. Ultrastructure of adult rd mouse retina. *Graefes Arch Clin Exp Ophthalmol*. 2003;241:410–417.
11. Jones BW, Watt CB, Frederick JM, et al. Retinal remodeling triggered by photoreceptor degenerations. *J Comp Neurol*. 2003;464: 1–16.
12. Leveillard T, Mohand-Said S, Lorentz O, et al. Identification and characterization of rod-derived cone viability factor. *Nat Genet*. 2004;36:755–759.
13. Streichert LC, Birnbach CD, Reh TA. A diffusible factor from normal retinal cells promotes rod photoreceptor survival in an in vitro model of retinitis pigmentosa. *J Neurobiol*. 1999;39:475–490.
14. Mohand-Said S, Deudon-Combe A, Hicks D, et al. Normal retina releases a diffusible factor stimulating cone survival in the retinal degeneration mouse. *Proc Natl Acad Sci USA*. 1998;95:8357–8362.
15. Mohand-Said S, Hicks D, Simonutti M, et al. Photoreceptor transplants increase host cone survival in the retinal degeneration (rd) mouse. *Ophthalmic Res*. 1997;29:290–297.
16. Steinberg RH. Survival factors in retinal degenerations. *Curr Opin Neurobiol*. 1994;4:515–524.
17. Shearstone JR, Wang YE, Clement A, et al. Application of functional genomic technologies in a mouse model of retinal degeneration. *Genomics*. 2005;85:309–321.
18. Hackam AS, Strom R, Liu D, et al. Identification of gene expression changes associated with the progression of retinal degeneration in the rd1 mouse. *Invest Ophthalmol Vis Sci*. 2004;45:2929–2942.
19. Rohrer B, Pinto FR, Hulse KE, Lohr HR, Zhang L, Almeida JS. Multidestructive pathways triggered in photoreceptor cell death of the rd mouse as determined through gene expression profiling. *J Biol Chem*. 2004;279:41903–41910.
20. Cavusoglu N, Thierse D, Mohand-Said S, et al. Differential proteomic analysis of the mouse retina: the induction of crystallin proteins by retinal degeneration in the rd1 mouse. *Mol Cell Proteomics*. 2003;2:494–505.
21. Corbo JC, Cepko CL. A hybrid photoreceptor expressing both rod and cone genes in a mouse model of enhanced S-cone syndrome. *PLoS Genet*. 2005;1:e11.
22. Young TL, Cepko CL. A role for ligand-gated ion channels in rod photoreceptor development. *Neuron*. 2004;41:867–879.
23. Turner DL, Snyder EY, Cepko CL. Lineage-independent determination of cell type in the embryonic mouse retina. *Neuron*. 1990;4: 833–845.
24. LaVail MM, Matthes MT, Yasumura D, Steinberg RH. Variability in rate of cone degeneration in the retinal degeneration (rd/rd) mouse. *Exp Eye Res*. 1997;65:45–50.
25. Jimenez AJ, Garcia-Fernandez JM, Gonzalez B, Foster RG. The spatio-temporal pattern of photoreceptor degeneration in the aged rd/rd mouse retina. *Cell Tissue Res*. 1996;284:193–202.
26. Treisman J, Morabito MA, Barnstable C. Opsin expression in the rat retina is developmentally regulated by transcription activation. *Mol Cell Biol*. 1988;8:1570–1579.
27. Morrow EM, Belliveau MJ, Cepko CL. Two phases of rod photoreceptor differentiation during rat retinal development. *J Neurosci*. 1998;18:3738–3748.
28. Chiu MI, Nathans J. A sequence upstream of the mouse blue visual pigment gene directs blue cone-specific transgene expression in mouse retinas. *Vis Neurosci*. 1994;11:773–780.
29. Szel A, Rohlich P, Mieziewska K, Aguirre G, van Veen T. Spatial and temporal differences between the expression of short- and middle-wave sensitive cone pigments in the mouse retina: a developmental study. *J Comp Neurol*. 1993;331:564–577.
30. Pacione LR, Szego MJ, Ikeda S, Nishina PM, McInnes RR. Progress toward understanding the genetic and biochemical mechanisms of inherited photoreceptor degenerations. *Annu Rev Neurosci*. 2003;26:657–700.
31. Wang Y, Macke JP, Merbs SL, et al. A locus control region adjacent to the human red and green visual pigment genes. *Neuron*. 1992; 9:429–440.
32. Blackshaw S, Harpavat S, Trimarchi J, et al. Genomic analysis of mouse retinal development. *PLoS Biol*. 2004;2:E247.
33. Carter-Dawson LD, LaVail MM, Sidman RL. Differential effect of the rd mutation on rods and cones in the mouse retina. *Invest Ophthalmol Vis Sci*. 1978;17:489–498.
34. Marc RE, Jones BW, Watt CB, Strettoi E. Neural remodeling in retinal degeneration. *Prog Retin Eye Res*. 2003;22:607–655.
35. Tsacopoulos M, Poitry-Yamate CL, MacLeish PR, Poitry S. Trafficking of molecules and metabolic signals in the retina. *Prog Retin Eye Res*. 1998;17:429–442.